# Magnetism without Magnetic Ions: Percolation, Exchange, and Formation Energies of Magnetism-Promoting Intrinsic Defects in CaO

J. Osorio-Guillén, S. Lany, S. V. Barabash, and A. Zunger*

*National Renewable Energy Laboratory, Golden, Colorado 80401, USA*

(Received 3 November 2005; published 14 March 2006)

We investigate theoretically the prospects of ferromagnetism being induced by cation vacancies in nonmagnetic oxides. A single Ca vacancy $V_{\mathrm{Ca}}^{0}$ has a magnetic moment due to its open-shell structure but the ferromagnetic interaction between two vacancies extends only to four neighbors or less. To achieve magnetic percolation on a fcc lattice with such an interaction range one needs a minimum of 4.9% vacancies, or a concentration $1.8 \times 10^{21}$ cm$^{-3}$. Total-energy calculations for CaO show, however, that due to the high vacancy formation energy even under the most favorable growth conditions one can not obtain more than 0.003% or $10^{18}$ cm$^{-3}$ vacancies at equilibrium, showing that a nonequilibrium vacancy-enhancement factor of $10^3$ is needed to achieve magnetism in such systems.

DOI: 10.1103/PhysRevLett.96.107203 PACS numbers: 75.50.Pp, 71.15.Mb, 71.55.−i, 75.10.−b

In addition to the magnetism manifested by *condensed* phases of magnetic atoms, such as solid elemental Fe or the FeNi compound, one encounters also collective magnetism promoted by *dilute* magnetic ions in nonmagnetic matrices [1], such as Mn in GaAs or CdTe and Gd in GaN. A special form of dilute magnets, forming a novel class of materials, is the case where nominal magnetic ions are not present, and the agents of dilute magnetism are said to be intrinsic lattice defects in the host matrix itself. Reported cases include Ca vacancy in CaO [2,3], Hf vacancy in $\mathrm{HfO_2}$ [4–6], or nonmagnetic impurities such as N and C in nonmagnetic CaO [3] or C in SrO [7]. Indeed, it has been shown theoretically [2], and known experimentally [8–10], that cation vacancies in ordinary oxides such as CaO [2] or MgO [9,10] have an open-shell electronic configuration, and thus carry a nonzero local magnetic moment. In fact, many point defects in ordinary semiconductors and insulators share the same properties of local moments. For example, the positively charged vacancy in Si has the orbital configuration $a_1^2 t_+^1 t_-^0$ (before Jahn-Teller relaxation) with magnetic moment of $1\mu_B$ [11], whereas the neutral Ga vacancy in GaP exhibits a $S = 3/2$ configuration $a_1^2 t_+^3 t_-^0$ $(3\mu_B)$ [12]. Yet these defected covalent systems are not known to exhibit *collective* magnetism, because the exchange coupling is presumably both weak and short ranged. For the ionic $\mathrm{HfO_2}$, the exchange coupling of pair of Hf vacancies was calculated theoretically [6] but it is unknown if the range of this interaction is sufficiently extended to sustain collective magnetism. Indeed, predicting and validating theoretically the exciting prospects that certain intrinsic defects would promote *collective ferromagnetism* in ordinary insulators and semiconductors requires a confluence of a few disciplines of condensed matter physics which will be illustrated here in the context of magnetism of CaO. This validation procedure, consisting of *four* steps, can be used for screening many interesting candidate systems of dilute magnetism without magnetic ions. The four issues are: (i) does the stable charge state of the isolated defect carry a magnetic moment? (ii) What is the range $d_{\max}$ of magnetic exchange interactions between a pair of defects in the stable charge states? (iii) Given $d_{\max}$, what is the minimum concentration $x_{\mathrm{per}}$ of defects in the stable charge state which will establish a continuous percolation (per) in the lattice? And finally (iv) can a minimum defect concentration $x_{\mathrm{per}}$ needed for magnetic percolation be granted thermodynamically given the calculated formation energy? We find here that the neutral charge state of a cation vacancy $V_{\mathrm{Ca}}^{0}$ in CaO does have a magnetic moment, that $d_{\max}$ is approximately four nearest neighbors, which requires a minimum concentration $x_{\mathrm{per}} = 4.9\%$ to establish percolation in this fcc sublattice. However, the high formation energy of $V_{\mathrm{Ca}}^{0}$ can yield only $x \leq 0.003\%$ at thermodynamic equilibrium even at high temperatures, falling short by over three orders of magnitude. Thus, a nonequilibrium enhancement factor $>10^3$ is needed to see vacancy-induced ferromagnetism in CaO.

We start by calculating the formation energy [13] $\Delta H(D^q, E_F, \mu)$ of defect $D$ in charge state $q$ (here, $D =$ Ca or O vacancies and $q = 0, \pm 1, \pm 2$) as a function of the Fermi energy $E_F$ and the chemical potential $\mu$ of Ca and O:

$$\Delta H(D^q, E_F, \mu) = [E(D^q) - E(\mathrm{H})] + (\mu_\alpha^{\mathrm{elem}} + \Delta\mu_\alpha) + q(E_v + \Delta E_F), \tag{1}$$

where $E(D^q)$ is the total energy of the semiconductor with the defect $D$ in charge state $q$, and $E(H)$ is the energy of the pure host. The second term describes the chemical reservoir in equilibrium, where the chemical potential $\mu_\alpha = \mu_\alpha^{\mathrm{elem}} + \Delta\mu_\alpha$ of the removed ion $\alpha (= \mathrm{Ca, O})$ is given with respect to the elemental phase. For the elemental reference $\mu_\alpha^{\mathrm{elem}}$, we choose the solid phase except for oxygen, where we use the $\mathrm{O_2}$ molecule. The third term in Eq. (1) is the energy of the electron reservoir, i.e., the Fermi energy $E_F = E_v + \Delta E_F$, which ranges from the valence band maximum $(E_v)$ to the conduction band minimum $(E_c)$

© 2006 The American Physical Society

and is determined by the equilibrium concentration of electrons and holes in the sample. Maintaining a system in thermodynamic equilibrium with bulk CaO requires $\mu_{\mathrm{Ca}} + \mu_{\mathrm{O}} = \mu_{\mathrm{CaO}}$, i.e., $\Delta\mu_{\mathrm{Ca}} + \Delta\mu_{\mathrm{O}} = \Delta H_f(\mathrm{CaO})$, where $\Delta H_f(\mathrm{CaO}) = -6.15$ eV is the calculated formation enthalpy of CaO. These leave one degree of freedom ($\mu_{\mathrm{Ca}}$ or $\mu_{\mathrm{O}}$) for the chemical potentials of the constituents. Thus, growth conditions can be chosen between the limit of Ca-poor [=O-rich, i.e., $\Delta\mu_{\mathrm{Ca}} = \Delta H_f(\mathrm{CaO})$, $\Delta\mu_{\mathrm{O}} = 0$] and the limit Ca-rich [=O-poor, i.e., $\Delta\mu_{\mathrm{Ca}} = 0$, $\Delta\mu_{\mathrm{O}} = \Delta H_f(\mathrm{CaO})$] conditions. Figure 1 gives the formation energies for these two extreme limits. All total energies are calculated via first-principles momentum-space pseudopotential method using the generalized gradient approximation (GGA) and the projector augmented wave method as implemented in the VASP code [14]. We next address the four questions posed above:

*(i) Does the stable charge state of the isolated defect carry a magnetic moment?*—The closed shell $V_{\mathrm{Ca}}^{2-}$ defect does not carry a magnetic moment. While we find for the singly charged $V_{\mathrm{Ca}}^{-}$ a magnetic moment of $1.0\mu_B$, and the neutral Ca vacancy $V_{\mathrm{Ca}}^{0}$ has a magnetic moment of $1.9\mu_B$. Thus, a spin-triplet ($S \approx 1$) configuration is found for $V_{\mathrm{Ca}}^{0}$. The $S = 1$ configuration has been observed experimentally in CaO and MgO, but the energy ordering between the spin-singlet ($S = 0$) and the spin-triplet states has been debated [8,10]. Based on EPR measurements for CaO the ground state was assigned tentatively to the spin singlet [8], and in MgO the ground state is a spin triplet [10]. In our GGA calculations for $V_{\mathrm{Ca}}^{0}$, the magnetic configuration ($m = 1.9\mu_B$) is lower in energy by 0.092 eV than the nonmagnetic ($m = 0\mu_B$) configuration. Other calculations also found that the spin-triplet is the ground state of $V^0$ [2,15]. Theoretically, this class of defects has been proposed to promote ferromagnetism [2,16–18].

The vacancy-projected and symmetry-decomposed local density of states, shown in Fig. 2, reveals that the electronic configuration is $(a_1^2 t_{1+}^3 e_+^2) t_{1-}^p e_-^q$, where the $e_-$ state is partially occupied ($q \approx 0.5$), leading to a transfer of some hole density to the $t_{1-}$ and $t_{2-}$ (the latter not shown) valence band states ($p \approx 2.5$). The corresponding hole density, obtained by integrating the two unoccupied states in the spin-down channel between $E_F$ and $E_F + 0.1$ eV (Fig. 2), is shown in the inset of Fig. 3. We see from Fig. 1 that under Ca-rich growth conditions the nonmagnetic defects of $V_{\mathrm{O}}^{q}$ and $V_{\mathrm{Ca}}^{2-}$ have a lower formation energy, hence, higher concentration than the magnetic defects $V_{\mathrm{Ca}}^{0}$ and $V_{\mathrm{Ca}}^{-}$ for all Fermi levels. In contrast, under Ca-poor conditions the magnetic species $V_{\mathrm{Ca}}^{-}$ and $V_{\mathrm{Ca}}^{0}$ are the stable defect states for $E_F \leq E_v + 0.68$ eV and for $E_F \leq E_v + 0.17$ eV, respectively. Therefore, in what follows we consider only Ca-poor growth conditions.

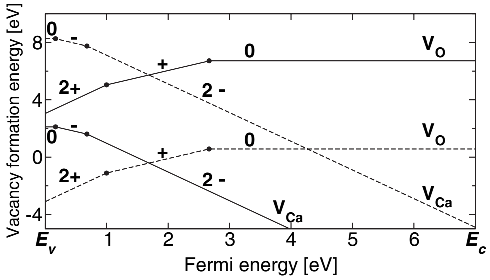

FIG. 1. Calculated formation enthalpies for anion and cation vacancies in CaO. Solid lines are for Ca-poor–O-rich ($\Delta\mu_{\mathrm{Ca}} = 0$ eV) chemical potentials whereas dashed lines are for Ca-rich–O-poor conditions ($\Delta\mu_{\mathrm{Ca}} = -6.15$ eV) chemical potentials. We have used the experimental gap $E_g = 7$ eV.

*(ii) What is the range $d_{\max}$ of magnetic exchange interactions between a pair of defects in the stable charge states?*—Since each $V_{\mathrm{Ca}}^{0}$ defect has a *partially* occupied orbital at $E_F$, the interaction between two such vacancies could lower the total energy if the spins are arranged ferromagnetically [19]. The energy lowering depends on the spatial extend and symmetry of the interacting states [19]. To quantify the ferromagnetic interaction we calculated the stabilization energy $\Delta E_{\mathrm{FM}}(d) = E_{\mathrm{FM}}(d) - E_{\mathrm{AFM}}(d)$ by placing two $V_{\mathrm{Ca}}^{0}$ defects at separation $d$ in the supercell and calculate via GGA the difference between the ferromagnetic (FM) and antiferromagnetic (AFM) total energies where all atomic positions are relaxed [20]. Figure 3 shows the resulting exchange energies $J_{ij}$ [21] for a 128-atom supercell. We see that the exchange energies vanish after the two defects are separated by $d_{\max} >$ four neighbors.

*(iii) Given $d_{\max}$, what is the minimum concentration $x_{\mathrm{per}}$ of defects in the stable charge state which will establish a*

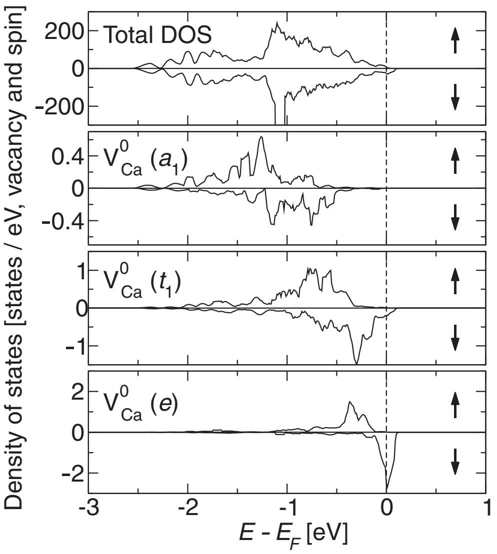

FIG. 2. Total density of states (DOS) and local DOS projected on a single neutral Ca-vacancy site (sphere radius = 2 Å) for the $\mathrm{Ca}_{63}V_{\mathrm{Ca}_1}\mathrm{O}_{64}$ supercell. The dashed line denotes the Fermi energy. Arrows pointing up (down) refer to up (down) spins. The total magnetic moment is $1.9\mu_B$.

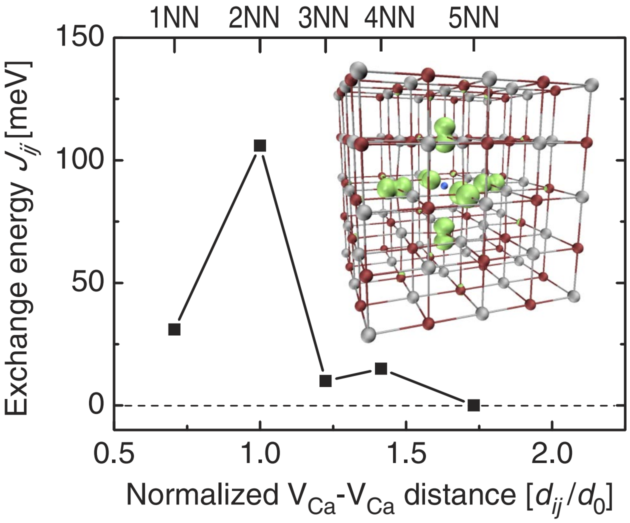

FIG. 3 (color online). Calculated exchange energies $J_{ij}$ for two neutral vacancies separated by distance $d_{ij}$ in CaO. The vacancy concentration is $x = 0.03125$, using a 128 atom supercell. The inset shows the hole density for the neutral $V_{Ca}^0$ (green isosurface: $0.02e/\text{Å}^{-3}$ calculated in the $Ca_{63}V_{Ca_1}O_{64}$ supercell). Ca and O ions are shown as gray and red spheres, respectively. The small blue sphere marks the site of the Ca vacancy.

*continuous percolation in the lattice?*—Figure 4(a) shows our calculated [22] percolation threshold concentration $x_{per}$ of the fcc lattice as a function of the normalized range $d_{ij}/d_0$ ($d_0$ is the CaO lattice constant) of interaction. We see that if the interaction range was limited to first fcc neighbors one would need a minimal concentration of 19.8% of vacancies to establish percolation, whereas if the interaction range is fourth fcc neighbors, a minimum concentration of 4.9% is needed to establish percolation. This corresponds to $1.8 \times 10^{21}$ atoms $\text{cm}^{-3}$. We next inquire if such a concentration can be granted, given the vacancy formation energies in Fig. 1.

*(iv) Can a minimum defect concentration $x_{per}$ needed for magnetic percolation be granted thermodynamically given the calculated formation energy?*—We calculate the concentration $x_{V_{Ca}}(T_g)$ under thermodynamic *equilibrium* at growth temperature $T_g$ (below the melting temperature $T_{melt} = 2900$ K of CaO), assuming that thermal quenching to room temperature freezes in the obtained concentrations at $T_g$. Since we are interested in maximizing the concentration of *magnetic* $V_{Ca}^0$, we choose growth conditions that minimize its formation energy Eq. (1), i.e., maximally Ca-poor conditions. At the same time, this minimizes compensation by $V_O$ formation which would yield nonmagnetic, charged $V_{Ca}^{2-}$ vacancies. In increasing degree of complexity and accuracy we present in Fig. 4(b) three models for the calculation of $x_{V_{Ca}}$:

(1) Neglecting the temperature and pressure dependence of the $O_2$ gas-phase chemical potential $\mu_{O_2}$, we take for the Ca-poor–O-rich regime $\mu_O^{elem} = 1/2\mu_{O_2}$ and $\Delta\mu_O = 0$ in Eq. (1), as done in conventional oxide calculations [23]. This approximation accounts for the use of the $T \to 0$ K limit for $1/2\mu_{O_2}(T, P)$, and yields $\Delta H(V_{Ca}^0) = 2.11$ eV. Using further an occupation probability according to the Boltzmann-factor, i.e., $x_{V_{Ca}} = x_{Ca-host}\exp(-\Delta H/k_BT)$, we obtain the curve labeled (1) in Fig. 4(b). In this model, the maximum attainable $V_{Ca}^0$ concentration is around $10^{19}$ $\text{cm}^{-3}$ at $T_g = T_{melt}$ or $x \approx 0.03\%$.

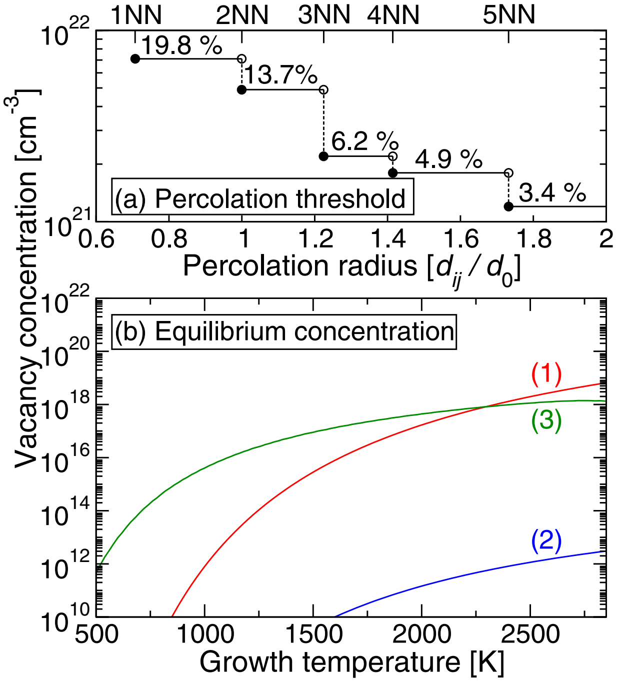

FIG. 4 (color online). (a) Calculated percolation radius vs vacancy concentration for a fcc lattice. (b) The equilibrium concentration of Ca vacancies $x(V_{Ca}^0)$ as a function of growth temperature $T_g$, under Ca-poor growth conditions using approximations (1)–(3) described in the text.

(2) We now include the enthalpy and entropy contributions to the oxygen chemical potential $\mu_O$ in the $O_2$ gas phase at temperature $T$ and pressure $P$. Using the tabulated [24] values for the $O_2$ standard ($T_0 = 298$ K, $P_0 = 1$ atm) enthalpy $H_0 = 8.7$ kJ $\text{mol}^{-1}$ and entropy $S_0 = 205$ J $\text{mol}^{-1}$ $\text{K}^{-1}$, we express $\Delta\mu_O$ in Eq. (1) as

$$\Delta\mu_O(T, P_0) = \tfrac{1}{2}\{[H_0 + \Delta H(T)] - T[S_0 + \Delta S(T)]\}, \quad (2)$$

where $\Delta H(T) = C_P(T - T_0)$ and $\Delta S(T) = C_P \ln(T/T_0)$. Employing the ideal gas law for $T \geq 298$ K, we use $C_P = 3.5k_B$ for the constant-pressure heat capacity per diatomic molecule. For pressures other than $P_0 = 1$ atm, one obtains $\mu_O(T, P) = \mu_O(T, P_0) + 1/2k_BT\ln(P/P_0)$ [25]. At ambient pressure, $P = 1$ atm, the gas-phase enthalpy and entropy contributions lower $\mu_O$ with respect to $1/2E_{tot}(O_2)$ by $\Delta\mu_O = -0.27$ eV at $T = 298$ K, and by as much as $\Delta\mu_O = -1.1$ eV already at $T = 1000$ K. Since thermodynamic stability of CaO requires $\mu_{Ca} + \mu_O = \mu_{CaO}$, the

Ca chemical potential $\mu_{\mathrm{Ca}}$ increases as $\mu_{\mathrm{O}}$ decreases with temperature, increasing the formation energy of $V_{\mathrm{Ca}}$ by the same amount [viz Eq. (1)]. Taking into account the temperature dependent $\Delta H(V_{\mathrm{Ca}}^0, T)$ and using $\Delta H(V_{\mathrm{Ca}}^0, T = 0\mathrm{K}) = 2.11$ eV as before, curve (2) in Fig. 4(b) shows the $V_{\mathrm{Ca}}^0$ concentration as a function of $T_g$. We see that the $O_2$ gas-phase enthalpy and entropy effects lead to a drastically reduced maximal $x_{V_{\mathrm{Ca}}^0} < 10^{13}\ \mathrm{cm}^{-3}$.

(3) In a final step, we take into account that both $V_{\mathrm{Ca}}$ and $V_{\mathrm{O}}$ can form, and both can exist in several charge states (Fig. 1). Since the formation energy $\Delta H(V_{\mathrm{Ca}})$ is reduced when $E_F$ rises in the band gap, due to formation of $V_{\mathrm{Ca}}^-$ and $V_{\mathrm{Ca}}^{2-}$ (viz Fig. 1), the total concentration $x_{V_{\mathrm{Ca}}}$ is much higher than that obtained under consideration of $V_{\mathrm{Ca}}^0$ only. We thus calculate the defect concentrations of $V_{\mathrm{Ca}}^0$ and $V_{\mathrm{Ca}}^-$ along with the equilibrium Fermi level in a self-consistent procedure [26], subject to the charge neutrality condition. Curve (3) in Fig. 4(b) shows for this model the calculated concentration of uncompensated, magnetic $V_{\mathrm{Ca}}^0$ rising above $10^{18}\ \mathrm{cm}^{-3}$ (0.003%) for $T_g \geq 2400$ K at $P_g = 1$ atm [Fig. 4(b)].

Comparing Figs. 4(a) and 4(b), we see that the highest possible equilibrium concentration of Ca vacancies (0.003%) fall considerably short of supplying the concentration of vacancies needed to achieve magnetic percolation in CaO (4.9%), even if we use the optimal chemical potentials during growth. We thus find that nonequilibrium thin film growth conditions would have to provide for an enhancement factor of about three orders of magnitude in the Ca-vacancy concentration relative to equilibrium growth in order to meet the percolation threshold.

In conclusion, we investigated the prospect of collective ferromagnetism mediated by intrinsic cation vacancy defects in CaO, using first-principles total-energy calculations. The employed comprehensive validation process covers the study of the magnetic properties of the isolated defects, the magnetic interaction of defect pairs and their range of interaction, and, finally, the thermodynamically generated defect concentrations. We find a substantial but short-ranged ferromagnetic coupling between Ca vacancies, requiring defect concentrations far in excess of thermodynamic equilibrium to achieve magnetic percolation.

This work was funded by DARPA under NREL Contract No. DE-AC36-99GO10337

---

*Email address: alex_zunger@nrel.gov
Electronic address: www.sst.nrel.gov

[1] *Diluted Magnetic Semiconductors*, edited by J. K. Furdyna and J. Kossut, Semiconductors and Semimetals Vol. 25 (Academic, New York, 1988).

[2] I. S. Elfimov, S. Yunoki, and G. A. Sawatzky, Phys. Rev. Lett. **89**, 216403 (2002).

[3] K. Kenmochi, M. Seike, K. Sato, A. Yanase, and H. Katayama-Yoshida, Jpn. J. Appl. Phys. **43**, L934 (2004).

[4] M. Venkatesan, C. B. Fitzgerald, and J. M. D. Coey, Nature (London) **430**, 630 (2004).

[5] J. M. D. Coey, M. Venkatesan, P. Stamenov, C. B. Fitzgerald, and L. S. Dorneles, Phys. Rev. B **72**, 024450 (2005).

[6] C. D. Pemmaraju and S. Sanvito, Phys. Rev. Lett. **94**, 217205 (2005).

[7] K. Kenmochi, V. A. Dinh, K. Sato, A. Yanase, and H. Katayama-Yoshida, J. Phys. Soc. Jpn. **73**, 2952 (2004).

[8] M. M. Abraham, Y. Chen, L. A. Boatner, and R. W. Reynolds, Solid State Commun. **16**, 1209 (1975).

[9] L. E. Halliburton, D. L. Cowan, W. B. J. Blake, and J. E. Wertz, Phys. Rev. B **8**, 1610 (1973).

[10] B. H. Rose and L. E. Halliburton, J. Phys. C **7**, 3981 (1974).

[11] G. D. Watkins, *Radiation Damage in Semiconductors* (Dunod, Paris, 1964).

[12] T. A. Kennedy, N. D. Wilsey, J. J. Krebs, and G. H. Stauss, Phys. Rev. Lett. **50**, 1281 (1983).

[13] C. Persson, Y.-J. Zhao, S. Lany, and A. Zunger, Phys. Rev. B **72**, 035211 (2005).

[14] G. Kresse and D. Joubert, Phys. Rev. B **59**, 1758 (1999).

[15] A. M. Stoneham, *Theory of Defects in Solids* (Clarendon, Oxford, 1975).

[16] M. Venkatesan, C. B. Fitzgerald, J. G. Lunney, and J. M. D. Coey, Phys. Rev. Lett. **93**, 177206 (2004).

[17] H. M. McConnell, Proceedings of the Robert A Welch Foundation Conferences on Chemical Research **11**, 144 (1967).

[18] C. Kollmar and O. Kahn, Acc. Chem. Res. **26**, 259 (1993).

[19] P. Mahadevan, A. Zunger, and D. D. Sarma, Phys. Rev. Lett. **93**, 177201 (2004).

[20] A Jahn-Teller-like symmetry breaking and hole localization is experimentally observed in the analogous MgO system (Ref. [10]), which is not reproduced by the present density functional calculations without self-interaction correction. Since, however, calculations at the GGA level do reproduce the coupling to a $S = 1$ triplet state (see Ref. [10]), we expect that the magnetic interactions are rather accurately represented.

[21] The exchange interaction energies are extracted from $\Delta E_{\mathrm{FM}}(d_{ij})$ via $J_{ij}(d_{ij}) = -(1/\lambda)\Delta E_{\mathrm{FM}}(d_{ij})$, where $\lambda$ is the number of equivalent pairs inside a sphere with chosen cutoff radius $d_{\max}$ such that $J_{ij}(d_{ij} > d_{\max}) = 0$.

[22] We determined the percolation thresholds, $x_{\mathrm{per}}$, for fcc lattices with interactions ranging up to the fifth nearest neighbor from Monte Carlo simulations using finite-size scaling analysis.

[23] A. F. Kohan, G. Ceder, D. Morgan, and C. G. van de Walle, Phys. Rev. B **61**, 15019 (2000); E. Lee, Y.-S. Kim, Y.-G. Jin, and K. J. Chang, Phys. Rev. B **64**, 085120 (2001).

[24] *CRC Handbook of Chemistry and Physics*, edited by R. C. Weast and M. J. Astle (CRC Press, Boca Raton, 1979), 60th ed.

[25] K. Reuter and M. Scheffler, Phys. Rev. B **65**, 035406 (2002).

[26] S. Lany, Y.-J. Zhao, C. Persson, and A. Zunger, Appl. Phys. Lett. **86**, 042109 (2005).